

Applications of nuclear reaction theory in medical radionuclide production

^{47}Sc production from enriched Titanium/nat Vanadium targets

F. Barbaro L. Canton, Y. Lashko, L. Zangrando

^{155}Tb production from enriched gadolinium targets

F. Barbaro, L. Canton, N. Uzunov, L. De Nardo, L. Melendez-Alafort

^{52}gMn production from natural Vanadium/Chromium targets

A. Colombi, M. P. Carante, F. Barbaro, L. Canton, A. Fontana, L. De Nardo, L. Melendez-Alafort



Istituto Nazionale di Fisica Nucleare

Padova



Istituto Nazionale di Fisica Nucleare

Legnaro



Padova



Padova

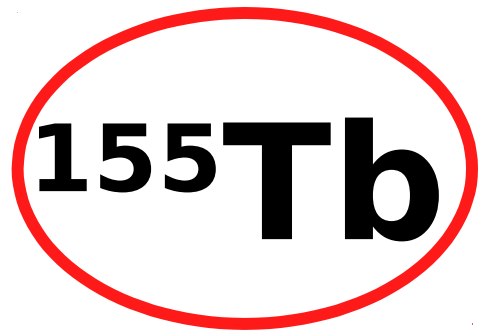


UNIVERSITÀ
DI PAVIA
Pavia



Kyiv

Within the REMIX Project: Research on the Emerging Medical radionuclides from the X-sections
Coordinated by **Gaia Pupillo** (INFN-LNL)



Which production route is adequate for clinical applications?

REMIX, METRICS projects of INFN-LNL
In collaboration with PD, MI, FE, PV...

Radiolotope	Half-life	Main Use	Additional Use	Context
^{47}Sc	3.35 d	β^- THERAPY	SPECT	Theranostic $^{44,43}\text{Sc}$
^{155}Tb	5.32 d	SPECT	AUGER THERAPY	Theranostic $^{149,152,161}\text{Tb}$
^{52g}Mn	5.59 d	PET	NMR	Multimodal Imaging

Main contaminants

^{46}Sc $T_{1/2} = 83.79$ d ; ^{48}Sc $T_{1/2} = 43.67$ h

^{156}Tb $T_{1/2} = 5.35$ d

^{54}Mn $T_{1/2} = 312.12$ d

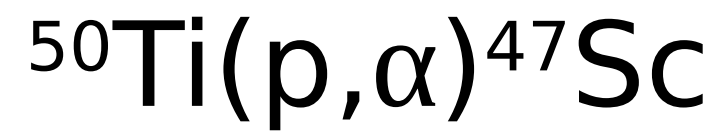
Preequilibrium models - in TALYS

- **PE 1 → Exciton model:** Analytical transition rates with energy-dependent matrix element
- **PE 2 → Exciton model:** Numerical transition rates with energy-dependent matrix element.
- **PE 3 → Exciton model:** Numerical transition rates with optical model for collision probability
- **PE 4 → Multi-step** direct/compound model
- **PE 5 → Geometry Dependent Hybrid (GDH)** model

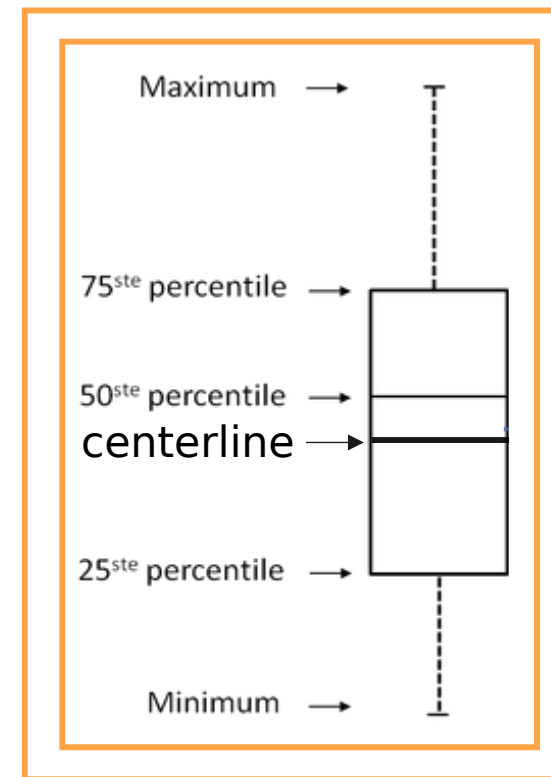
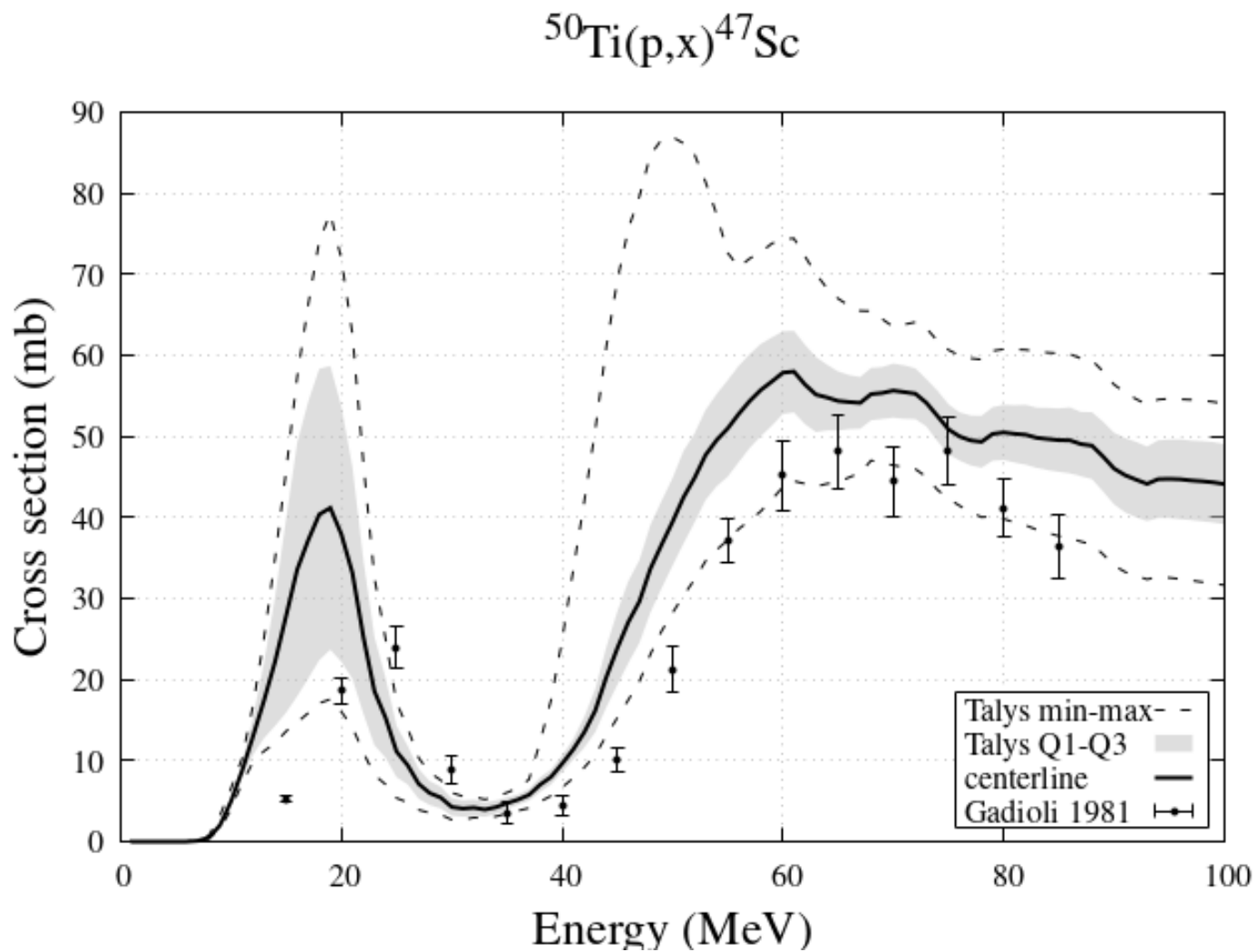
from TALYS-G implementation provided by KIT

Level density models - in TALYS

- LD 1 → Constant temperature + Fermi gas model
 - LD 2 → Back-shifted Fermi gas model
 - LD 3 → Generalised superfluid model
- phenomenological**
- LD 4 → Microscopic level densities (Skyrme force) from Goriely's tables
 - LD 5 → Microscopic level densities (Skyrme force) from Hilaire's combinatorial tables
 - LD 6 → Microscopic level densities (temperature dependent HFB, Gogny force) from Hilaire's combinatorial tables
- microscopic**

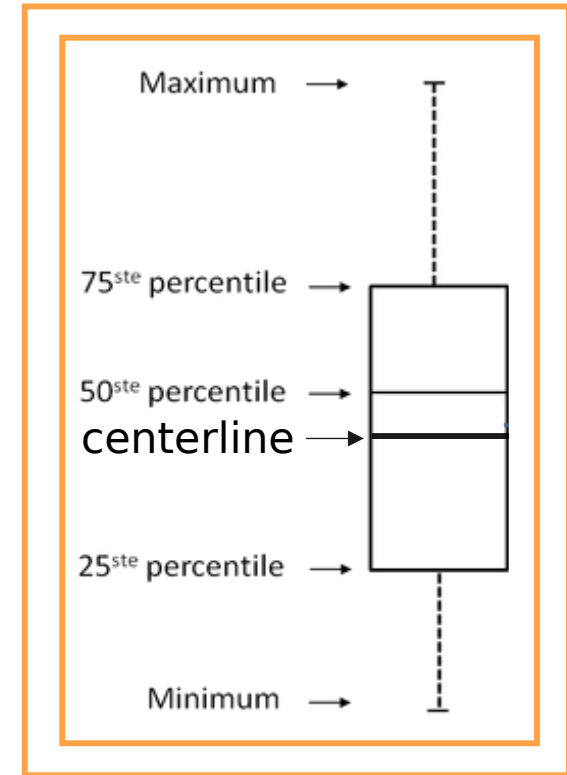
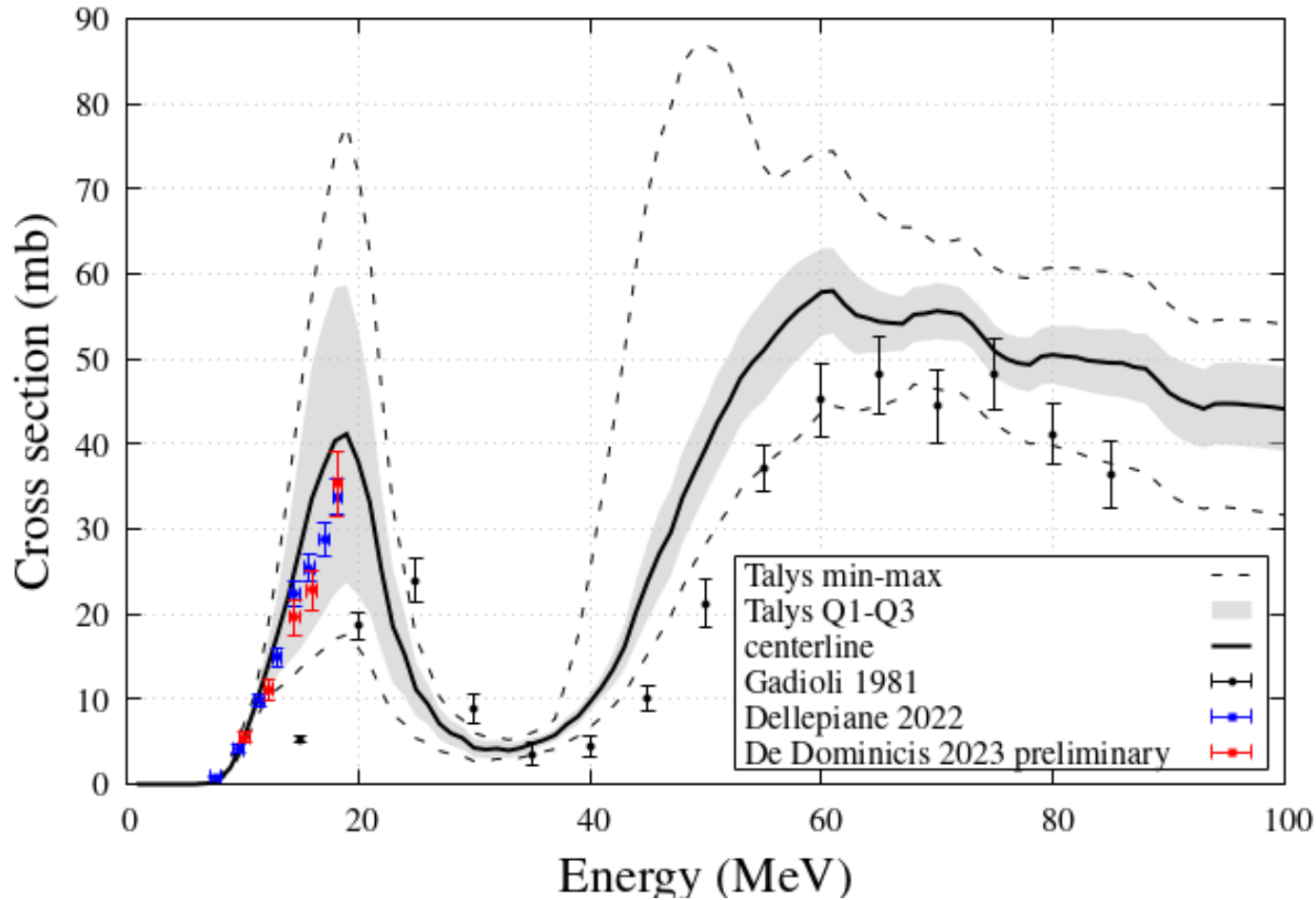
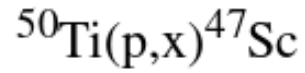


Representing the model variability of Talys calculations



Box-Whisker Plot

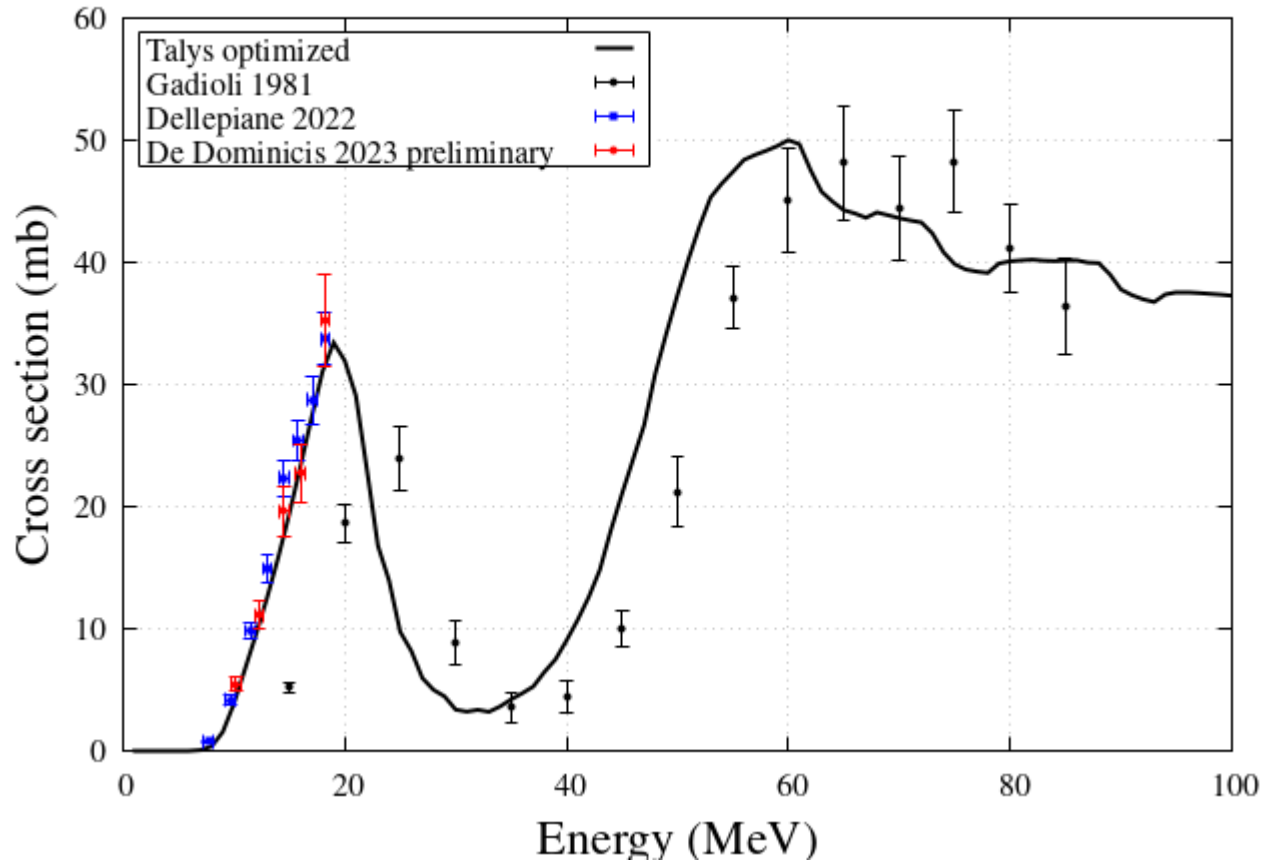
The new experimental data are very promising!



Box-Whisker Plot

Optimization of level density parameters to get curves guided by data

$^{50}\text{Ti}(p,x)^{47}\text{Sc}$



$$\rho(E) = \exp(c\sqrt{E - p})\rho(E - p)$$

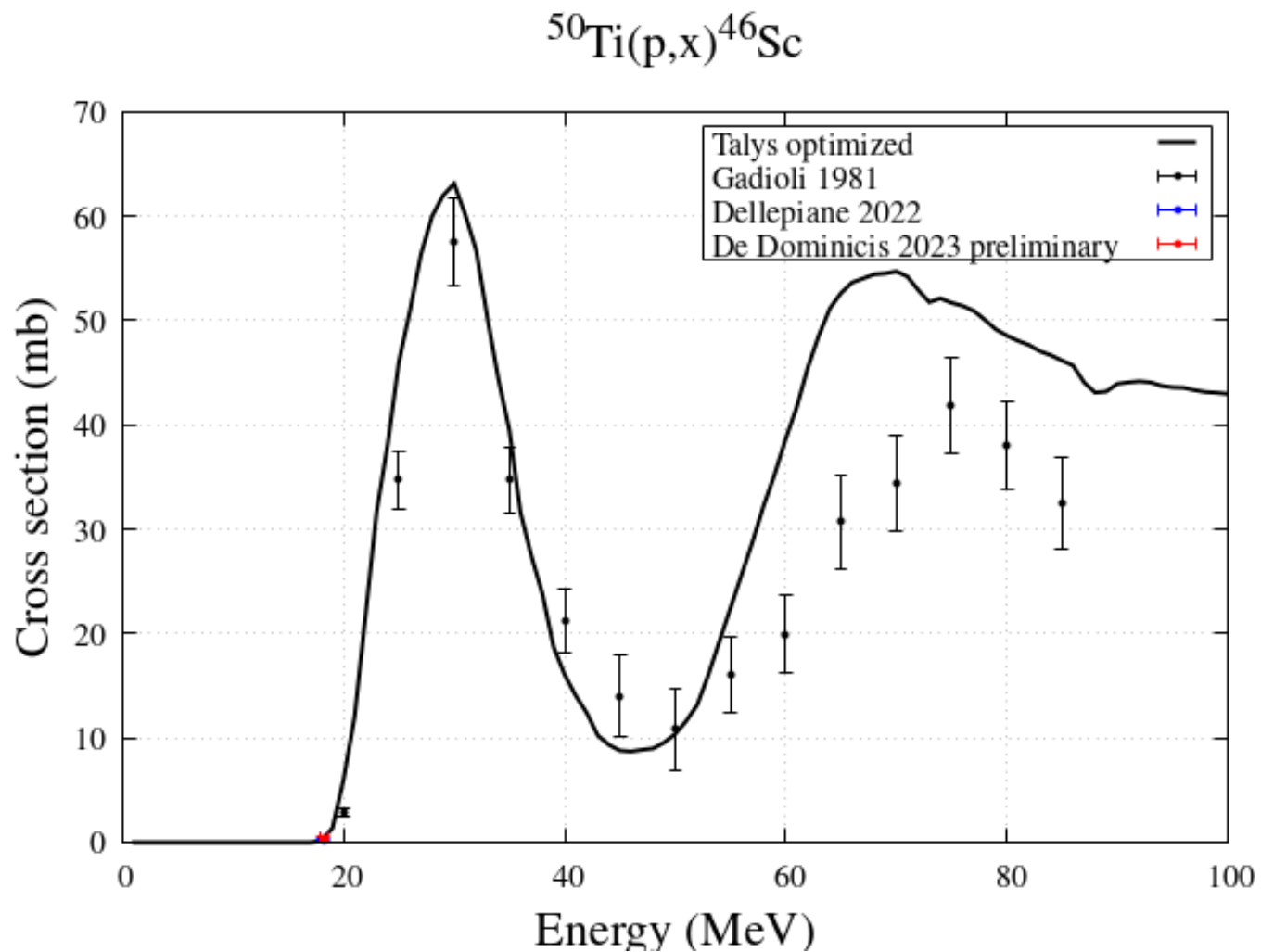
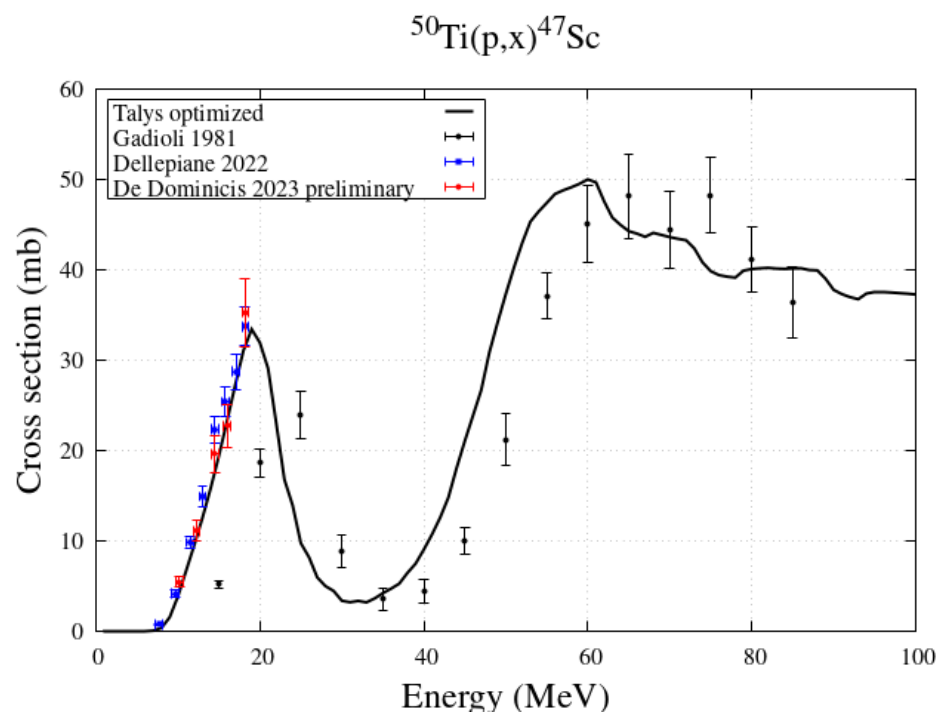
Modified level density
of ^{47}Sc compound



PE 3 - LD 4

$$c = 0.0 \text{ MeV}^{-1/2}$$
$$p = 0.5 \text{ MeV}$$

... and contaminants cross-sections



From Cross-Sections to Yields and RNP Purities

Production rate

$$R = \frac{I_0}{z_{proj} |e|} \frac{N_A}{A} \int_{E_{out}}^{E_{in}} \sigma(E) \left(\frac{dE}{\rho_t dx} \right)^{-1} dE$$

Bateman equations

$$\frac{dN_i}{dt} = R_i - \lambda_i N_i + \sum_{j < i} f_{ij} \lambda_j N_j$$

activities

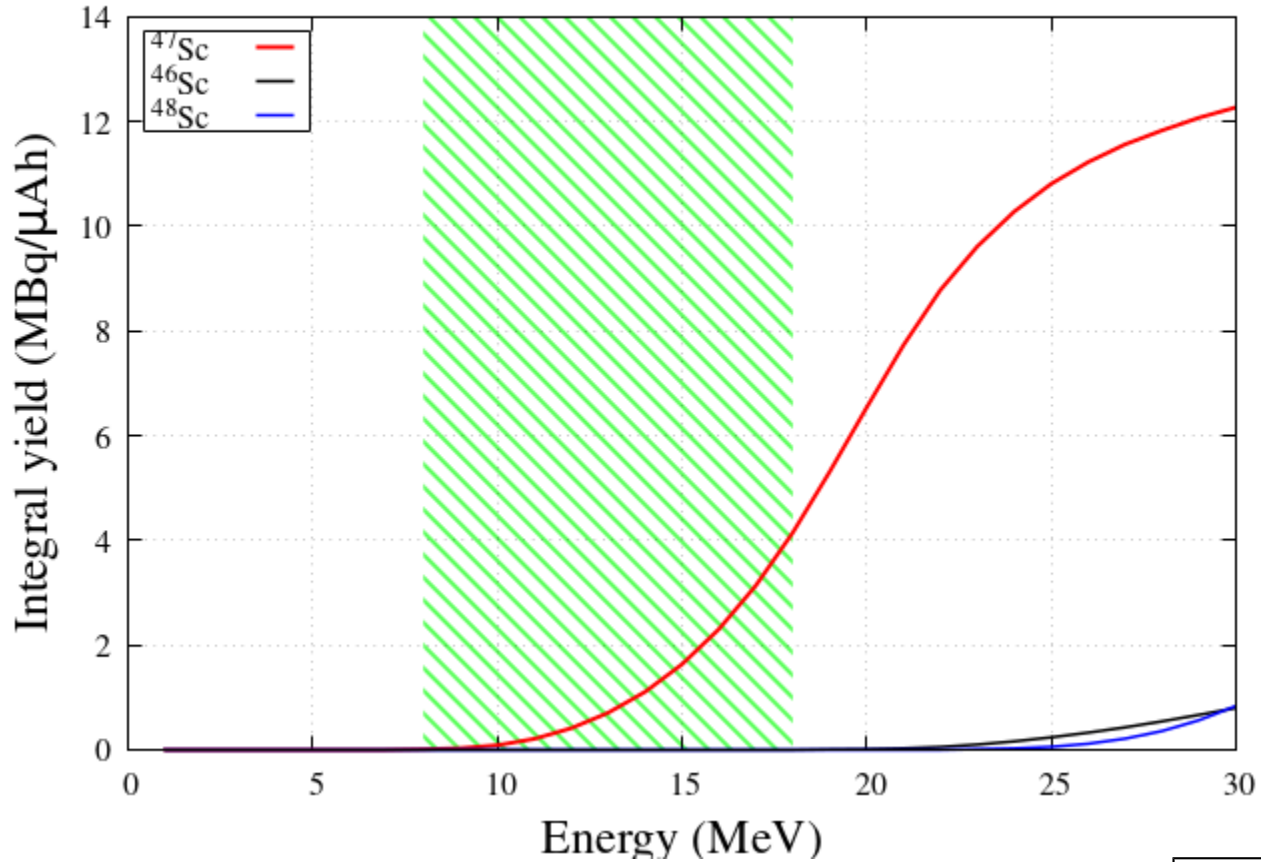
$$A_i(t) = \lambda_i N_i(t)$$

purities

$$RNP(t) = \frac{A_{*x}(t)}{\sum_i A_{ix}(t)}$$

Significant Yield of ^{47}Sc

$^{50}\text{Ti}(p,x)^{47/46/48}\text{Sc}$ Integral yield



Irradiation conditions

$$t_{\text{irr}} = 1 \text{ h}$$

$$i = 1 \text{ } \mu\text{A}$$

$$E_{\text{max}} = 18 \text{ MeV}$$

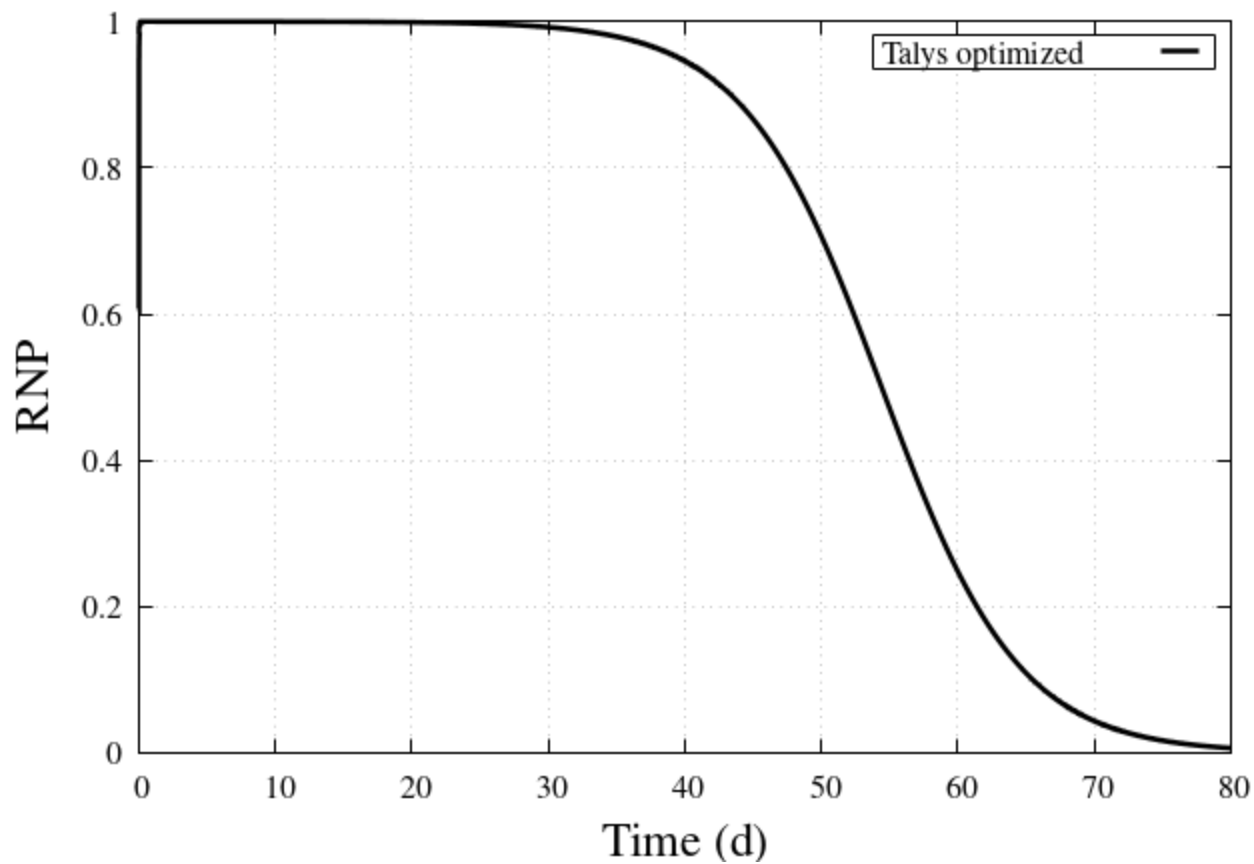
$$E_{\text{min}} = 8 \text{ MeV}$$

Yield (MBq/(μA·h))		
^{47}Sc	^{46}Sc	^{48}Sc
4.138	8.35E-05	0.0

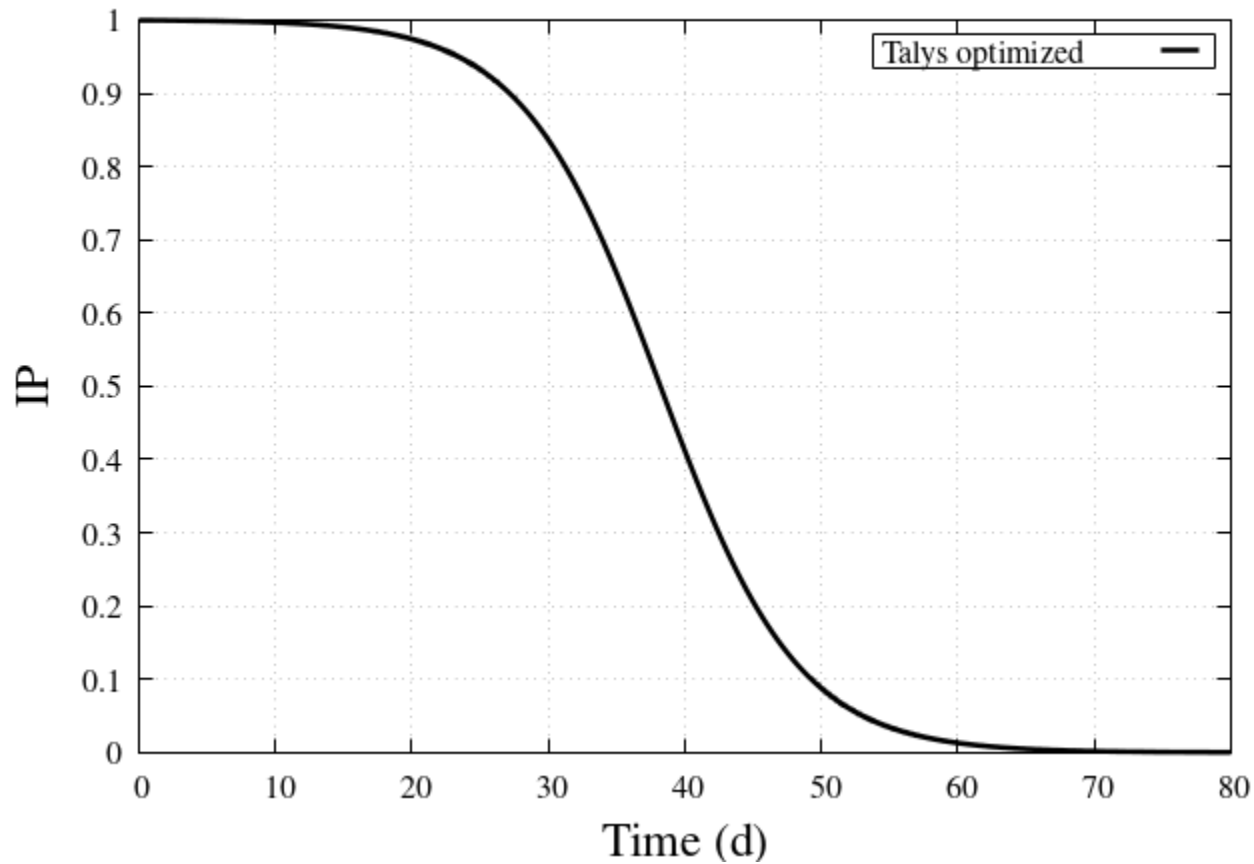
$$\text{RNP} = \frac{A^{47\text{Sc}}}{\sum_i A_i}$$

$$\text{IP} = \frac{n^{47\text{Sc}}}{\sum_i n_i}$$

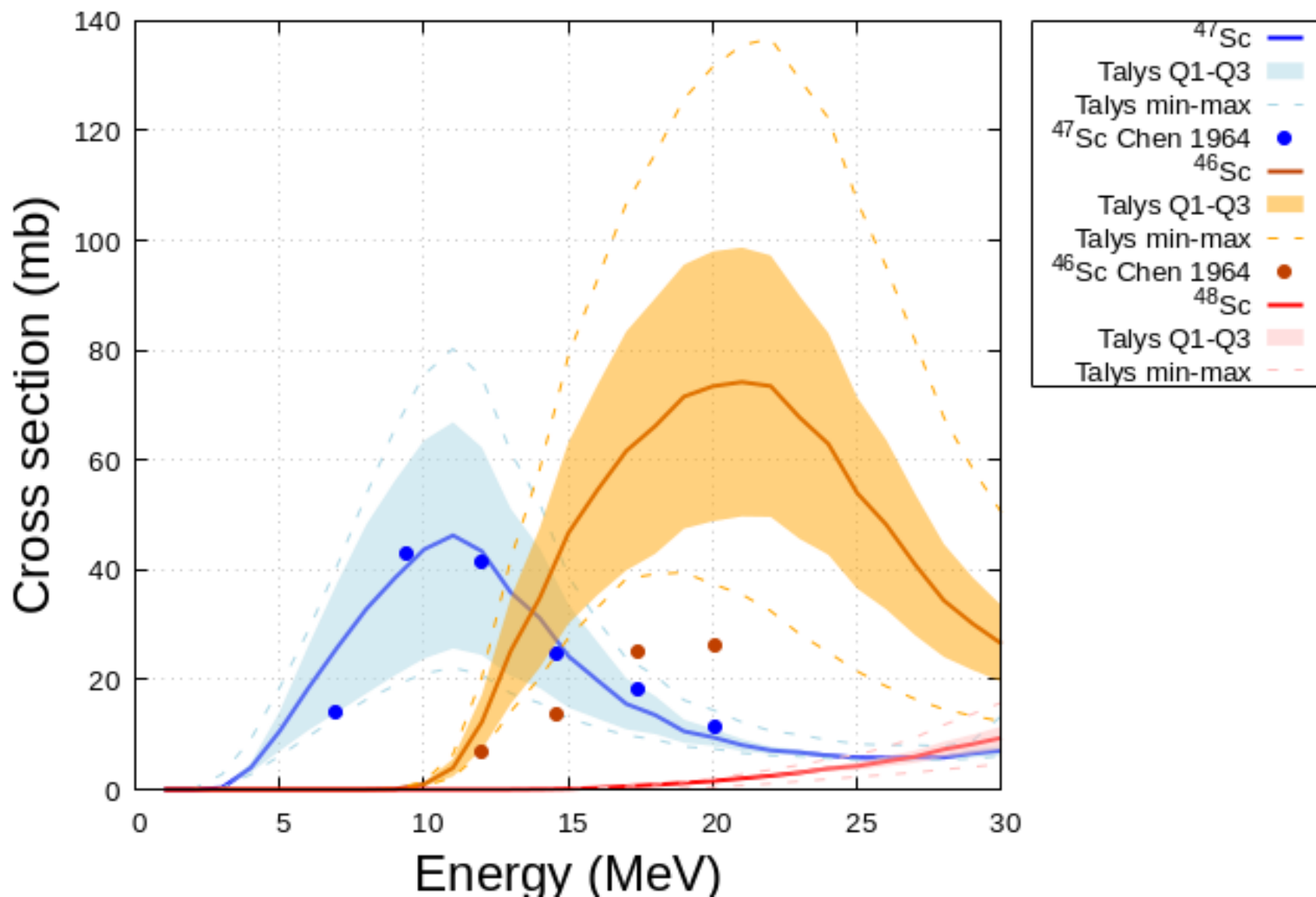
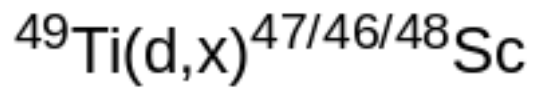
$^{50}\text{Ti}(\text{p},\text{x})^{47}\text{Sc}$ Radio Nuclidic Purity



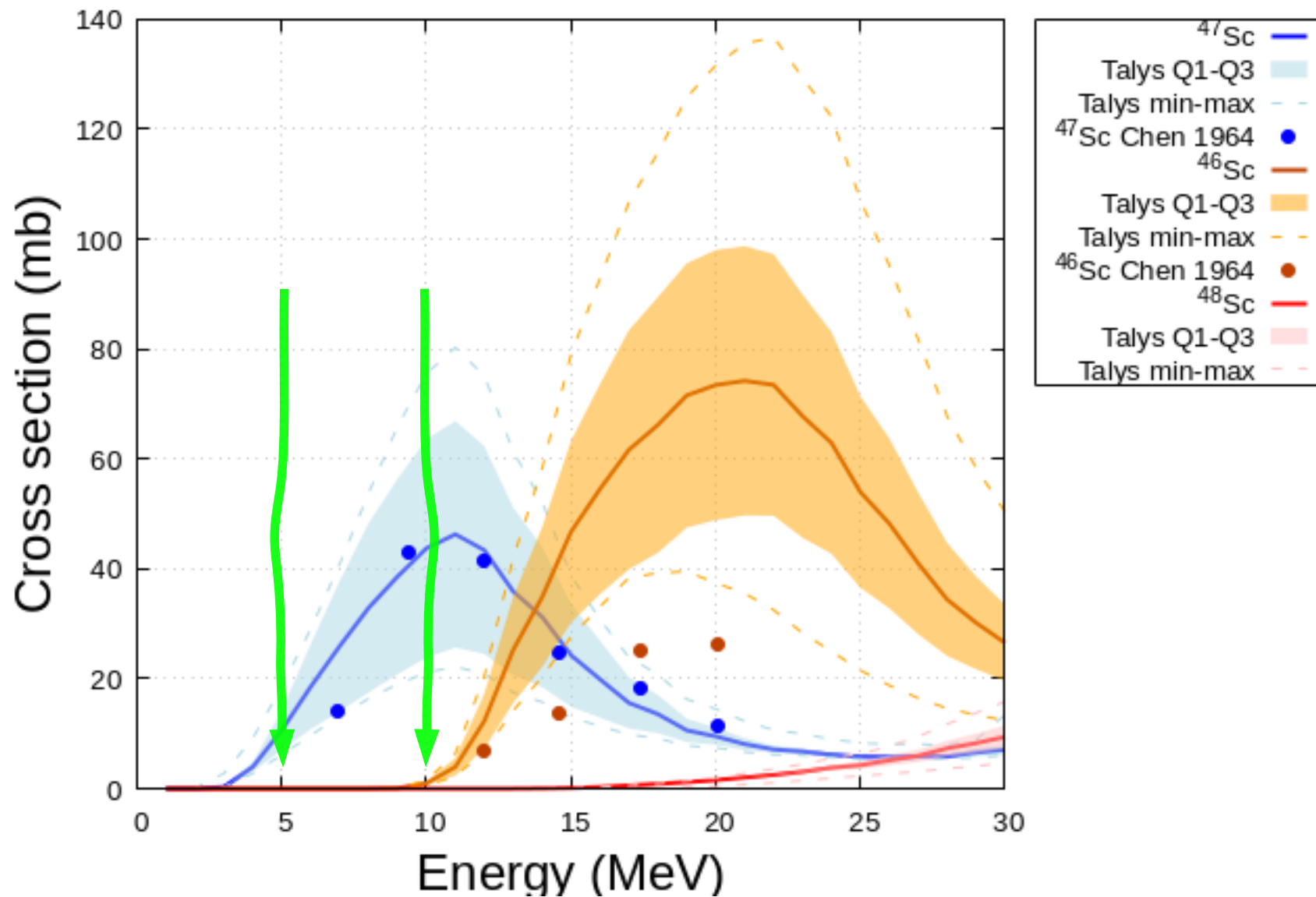
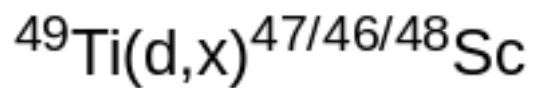
$^{50}\text{Ti}(\text{p},\text{x})^{47}\text{Sc}$ Isotopic Purity





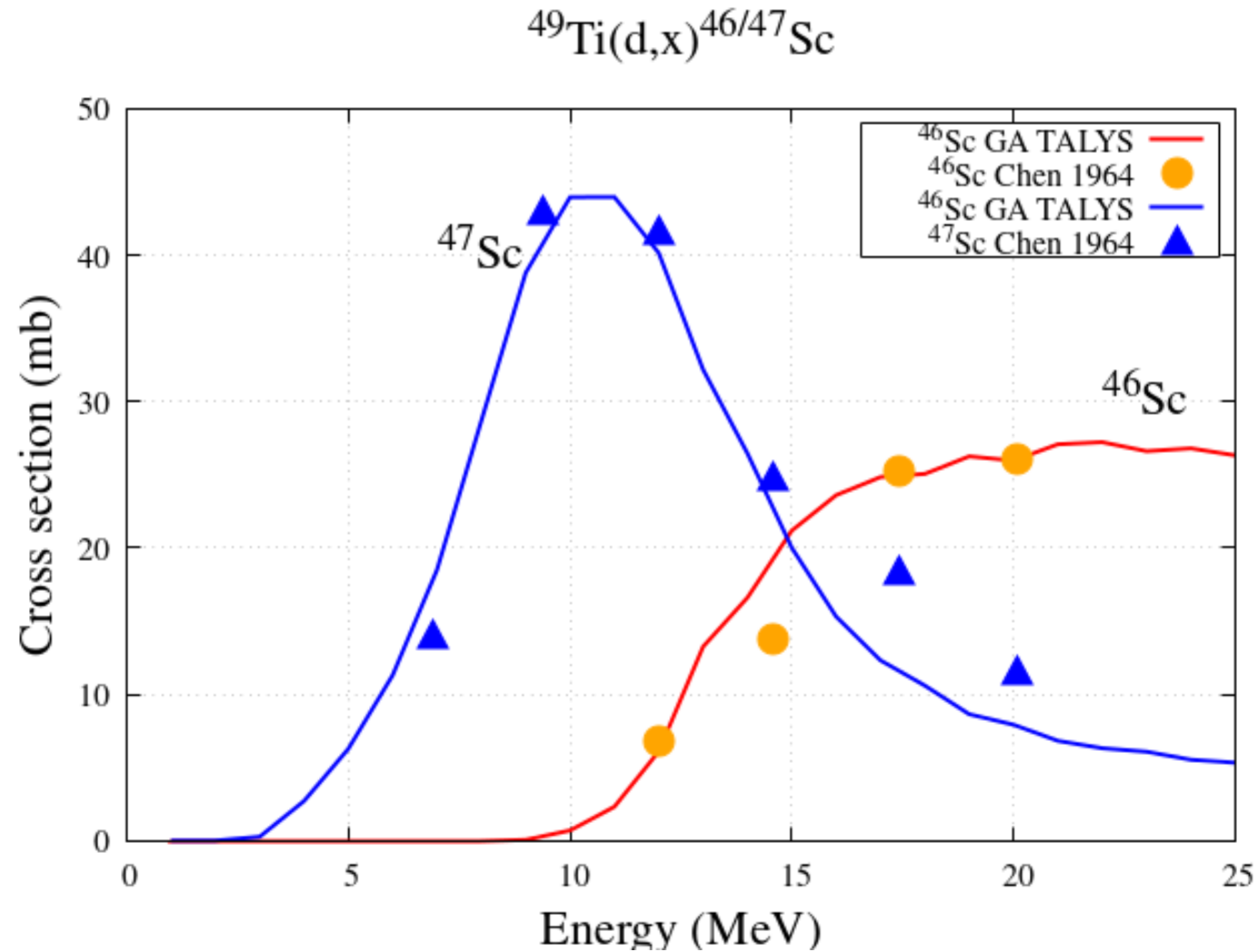


Model variability in TALYS



Promising route below 10 MeV

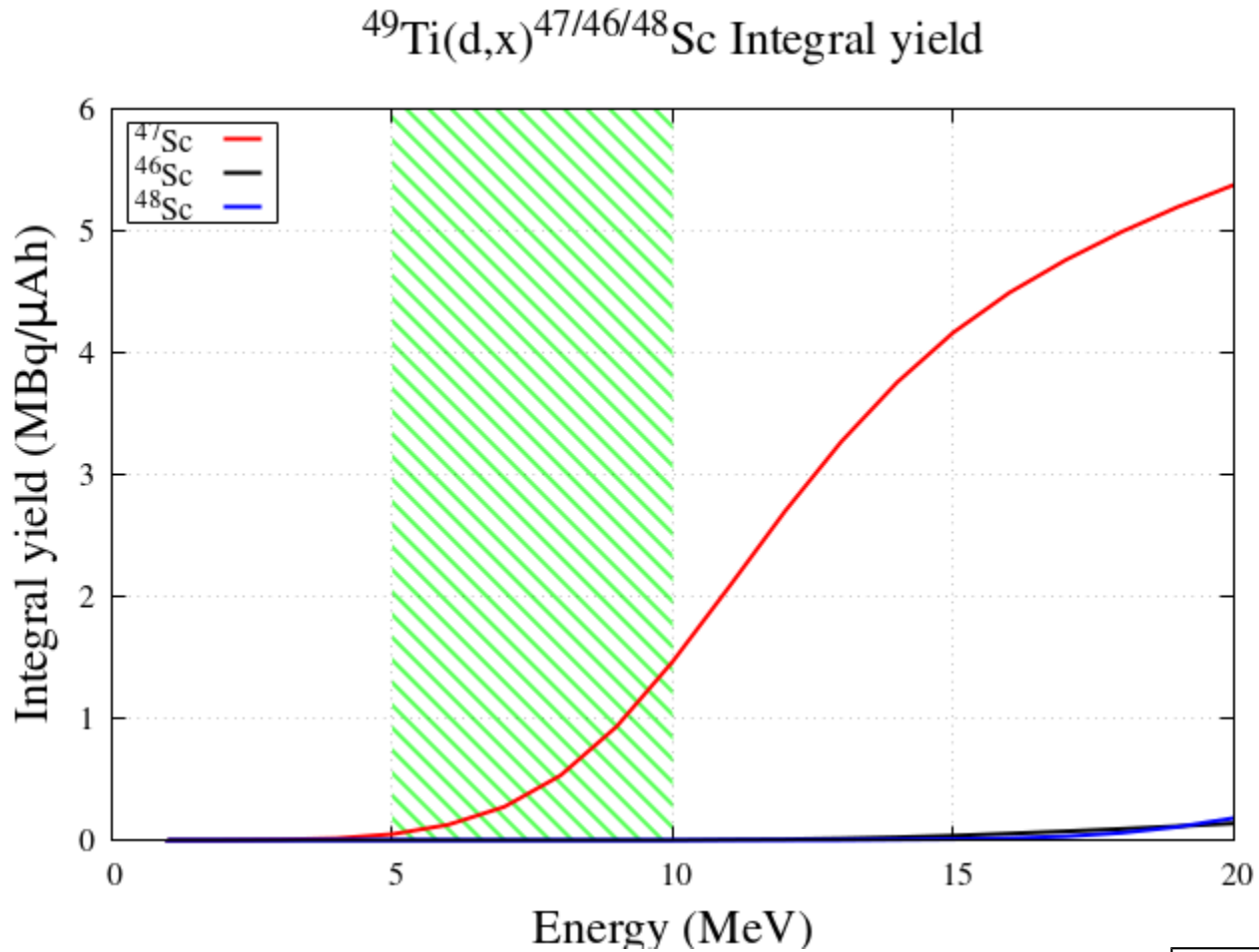
Optimization by genetic algorithms



PE 3 - LD 6

$$\begin{cases} ^{46}\text{Sc} & c = 1.573 \text{ MeV}^{-1/2}, p = 0.390 \text{ MeV} \\ ^{47}\text{Sc} & c = -0.029 \text{ MeV}^{-1/2}, p = 1.327 \text{ MeV} \end{cases}$$

Yield



Irradiation conditions

$$t_{\text{irr}} = 1 \text{ h}$$

$$i = 1 \mu\text{A}$$

$$E_{\text{max}} = 10 \text{ MeV}$$

$$E_{\text{min}} = 5 \text{ MeV}$$

Yield (MBq/($\mu\text{A}\cdot\text{h}$))		
^{47}Sc	^{46}Sc	^{48}Sc
1.418	2.14E-04	0.0

Conclusions

arxiv.org/abs/2310.02825

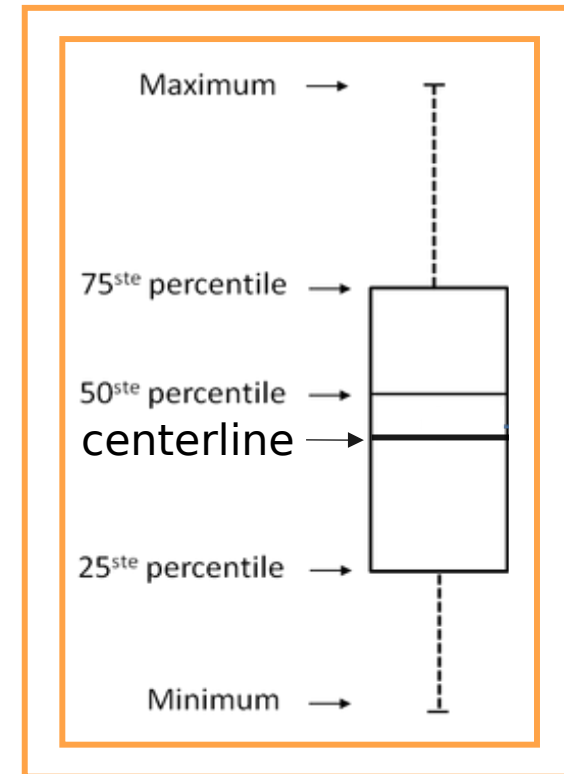
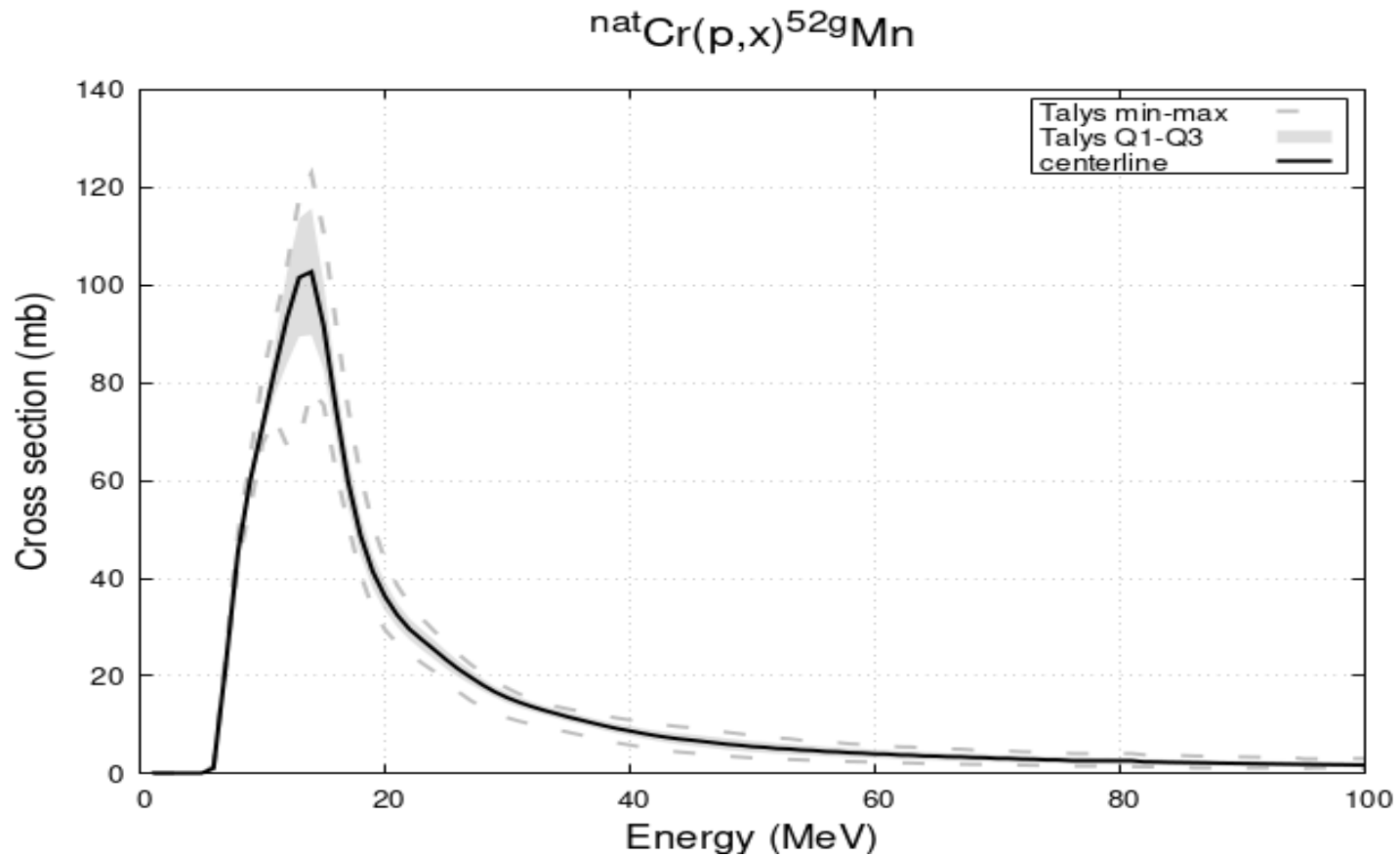
Both $^{50}\text{Ti}(p,\alpha)^{47}\text{Sc}$ and $^{49}\text{Ti}(d,\alpha)^{47}\text{Sc}$ are promising routes for hospital-cyclotron production

- ✓ High purity (RNP >99%)
- ✓ Yield 4.1 MBq/($\mu\text{A}\cdot\text{h}$) for $^{50}\text{Ti}(p,\alpha)$ @ 18 MeV
 1.4 MBq/($\mu\text{A}\cdot\text{h}$) for $^{49}\text{Ti}(d,\alpha)$ @ 10 MeV

$^{50}\text{Ti}(p,\alpha)$ → The new data by Dellepiane 2022 and the – still preliminary – confirmation 2023 by REMIX experiment (Pupillo, Mou, De Dominicis etc) changed dramatically the perspectives for this reaction, in positive!

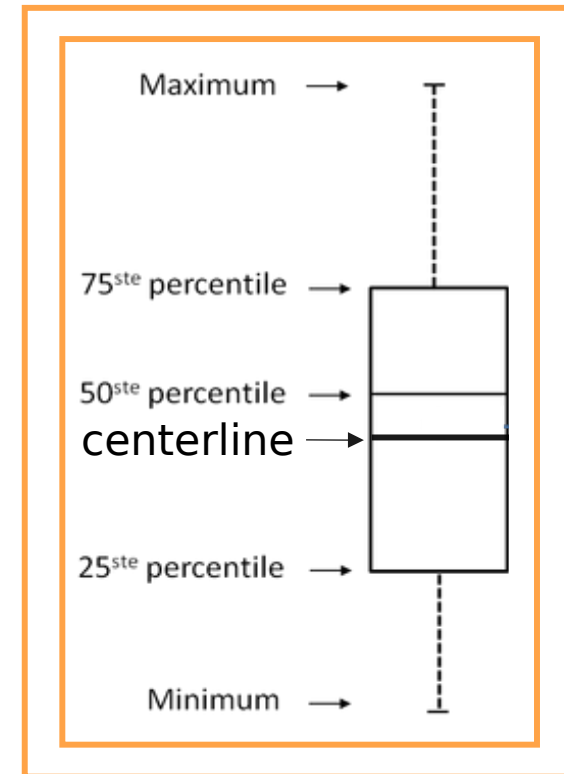
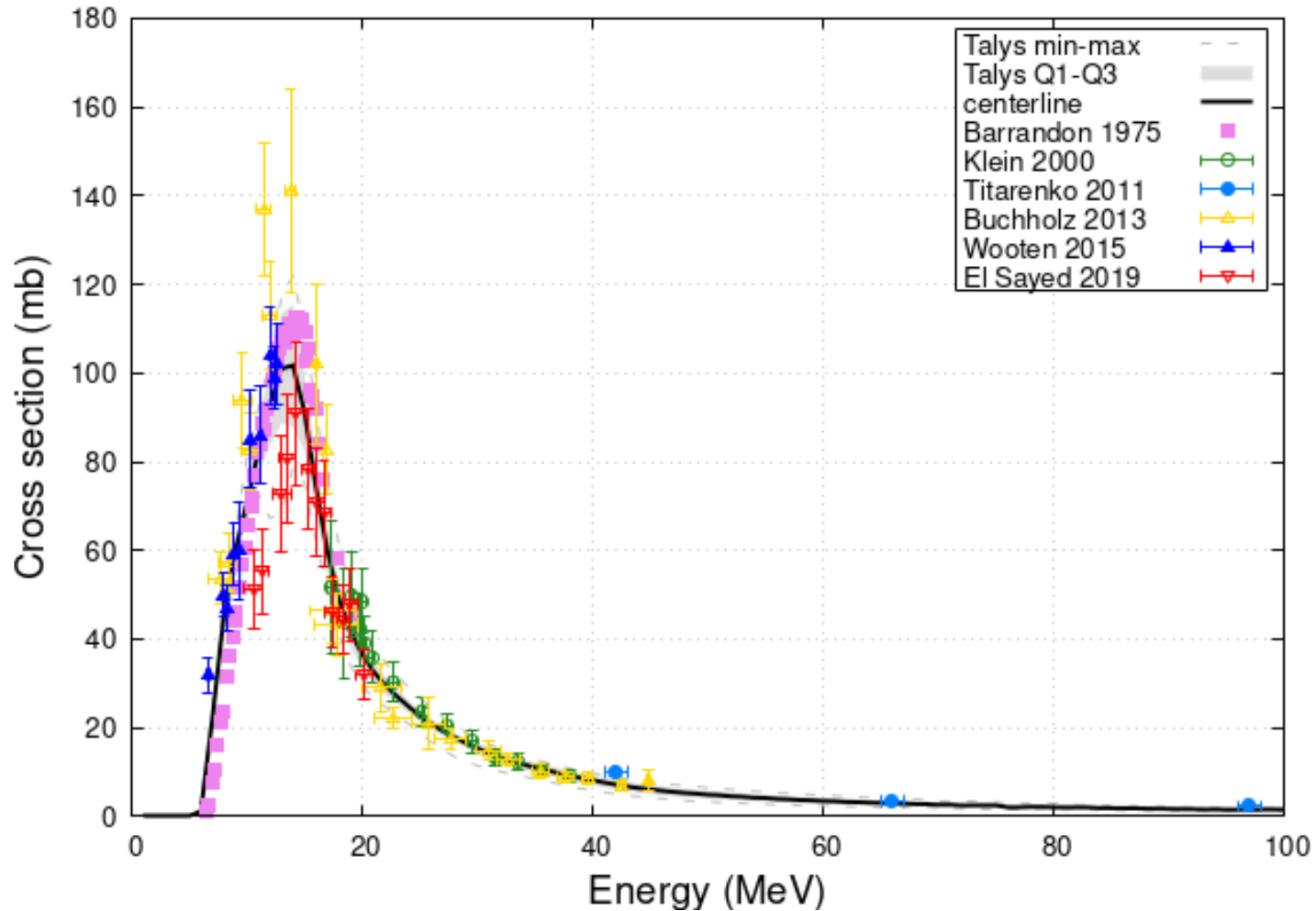
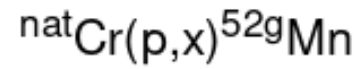
$^{49}\text{Ti}(d,\alpha)$ → Promising but the 1964 data by Cheng need to be confirmed!

Representing the model variability of TALYS calculations



Box-Whisker Plot

Not always the model dispersion is large !



Box-Whisker Plot